Substituent Effect on the Spin-trapping Reactions of Substituted *N*-Benzylidene-t-butylamine *N*-Oxides

Katsumi Murofushi, Kazuhisa Abe, and Minoru Hirota *
Department of Applied Chemistry, Faculty of Engineering, Yokohama National University, Hodogaya-ku, Yokohama 240, Japan

Relative rates of the reactions of substituted *N*-benzylidene-t-butylamine *N*-oxides with substituted phenyl free radicals have been determined by e.s.r. spectroscopic analyses of the products from competitive addition reactions. The substituent effect was interpreted in terms of a reaction mechanism involving an electron-transfer interaction between the reactants. The results are in accord with semi-empirical MO calculations.

Although many organic reactions are known to proceed *via* free radical intermediates[1,2] it is very difficult to detect and identify such species by routine chemical and physical methods. Involvement of free radicals in reactions is often deduced by analogy with established free radical reactions and from theoretical calculations. An important technique to indirectly identify short-lived organic free radicals is spin-trapping. This method was first developed by Janzen and co-workers[3,4] and has been applied to radiation chemistry,[5] biochemistry,[6] and polymer chemistry.[7] Nitrones and nitroso compounds are the most common spin traps, or spin-trapping reagents, and are designed to generate nitroxide free radicals on reaction with short-lived free radicals.[8,9]

N-Benzylidene-t-butylamine *N*-oxide (abbreviated as PBN after its common name phenyl t-butyl nitrone) is one of the most versatile spin traps, and the polar substituent effect on the reactions of a series of substituted PBNs towards hex-5-enyl free radicals has been studied kinetically by Schmid and Ingold.[10] These workers found that electron-withdrawing groups enhanced the rate of alkyl addition and *vice versa* to give ρ 0.2. Polar substituents effects were also reported on several free radical reactions, mostly abstraction reactions, of alkyl free radicals towards a series of substituted toluenes and shown to give Hammett plots with positive ρ-values.[11–14] In contrast, a negative ρ-value was reported for the reaction of the t-butoxyl free radical towards substituted toluenes.[15] The results have been interpreted by taking into account the electron-donating and -withdrawing contribution in the transition state. The above results suggest the participation of an electron-transfer interaction leading to intermediary formation of a charge-transfer complex between the free radical and the substrate in the course of the free-radical reactions.

In this investigation, the reactions between several substituted PBNs and substituted phenyl free radicals were studied by e.s.r. spectroscopy in order to examine the nature of the transition state. The experimental data, as well as theoretical results from MO calculations, support a mechanism involving the electron-transfer interaction between the free radical and the nitrone in an early and rate-determining stage of the reaction.

Results and Discussion

Relative Rates of Spin-trapping Reactions of Substituted N-*Benzylidene-t-butylamine* N-*Oxides with Substituted Phenyl Free Radicals.*—Rate constants of spin-trapping reactions have been determined either by examining two competing reactions of the same order or by comparison with reactions of known rate constants.[10] The relative reactivities of substituted *N*-benzylidene-t-butylamine *N*-oxides (X–PBN) towards an aryl free radical ($YC_6H_4^{\bullet}$) were evaluated using as reference the competitive reaction with *N*-benzylidene[$^2H_5$]aniline *N*-oxide ([$^2H_5$]DPN).[16,17]

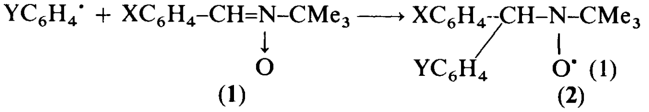

$$YC_6H_4^{\bullet} + \underset{(1)}{\underset{O}{\underset{\downarrow}{XC_6H_4\text{–}CH{=}N\text{–}CMe_3}}} \longrightarrow \underset{(2)}{XC_6H_4\text{–}\underset{YC_6H_4}{CH}\text{–}\underset{O^{\bullet}}{N}\text{–}CMe_3} \quad (1)$$

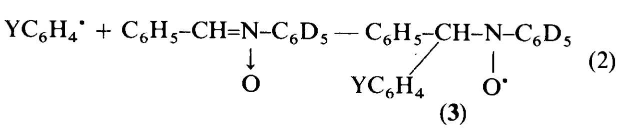

$$YC_6H_4^{\bullet} + \underset{O}{\underset{\downarrow}{C_6H_5\text{–}CH{=}N\text{–}C_6D_5}} — \underset{(3)}{C_6H_5\text{–}\underset{YC_6H_4}{CH}\text{–}\underset{O^{\bullet}}{N}\text{–}C_6D_5} \quad (2)$$

Concentrations of the formed spin adducts [**2**] and [**3**] can be correlated with the relative rate constant as given in equation (3).

$$\frac{k_1}{k_2} = \frac{[\mathrm{DPN}]\,(\mathrm{d}[\mathbf{2}]/\mathrm{d}t)_{t\to 0}}{[\mathrm{X\text{–}PBN}]\,(\mathrm{d}[\mathbf{3}]/\mathrm{d}t)_{t\to 0}} \quad (3)$$

The ratio of spin adducts ([**2**]/[**3**]) was measured at an early stage of the reaction in order to determine the relative rate of the spin-trapping reaction. Use of [$^2H_5$]DPN instead of unlabelled DPN eliminates undesirable overlapping of the hyperfine splitting lines caused by phenyl.[18] The method is effective in determining the relative rate constants for reactions of substituted X–PBNs with aryl free radicals ($YC_6H_4^{\bullet}$) (Table 1). In order to examine the substituent effect on the rate of the spin-trapping reaction[19] (1) logarithms of the relative rate constants were plotted against the Hammett σ-constants[20,21] (Figure 1). The reaction constants (ρ) of the plots and their reliability constants (r) are given in Table 2. In general, the rate constants correlate with the Hammett σ values of the substituent (X) on PBN, though the absolute ρ values are rather small. The Hammett law was shown to be applicable to reactions in which electronegative free radicals such as bromine ($Br^{\bullet}$) and trichloromethyl ($^{\bullet}CCl_3$) are involved.[18,22] Thus, the conformity to the Hammett law is suggestive of a mechanism in which charge separation plays an important role. The plot has a negative slope when the substituent (Y) on the phenyl free radical is electron-withdrawing and a positive slope when it is electron-donating. In other words, an electron-rich aryl free radical interacts favourably with an electron-deficient spin trap, and *vice versa*.

The tendency of the substituent effect is anticipated if we assume an electron-transfer interaction between the aryl free radical and the substituted PBN in the transition state. To rationalize the observed substituent effect by assuming the transitory formation of a charge-transfer complex, INDO-MO

Table 1. Rate constants of the spin-trapping reactions relative to reactions with the unsubstituted nitrone (X = H)

		X									
Y		4-MeO	4-Me	3-Me	H	4-F	3-MeO	4-Cl	3-Cl	3-NO_2	4-NO_2
4-Me	b	0.57	0.74	0.76	1.00	1.10	1.17	1.27	1.21	1.58	1.63
	a	0.57	0.80	0.75	1.00	1.21	0.99	1.22	1.23	1.33	1.40
3-Me	b	0.68	0.94	1.04	1.00	1.01	1.01	1.04	1.14	1.30	1.14
H	b	0.72	0.92	0.96	1.00	0.89	0.84	0.82	0.75	0.58	0.63
	a	0.96	0.72	0.85	1.00	0.74	0.75	0.75	0.67	0.63	0.72
4-F	b	1.19	1.33	1.11	1.00	0.79	0.86	0.75	0.79	0.71	0.71
	a	1.21	1.21	1.07	1.00	0.84	0.79	0.77	0.79	0.65	0.64
4-Cl	b	1.02	1.23	1.03	1.00	0.78	0.89	0.76	0.70	0.67	0.59
	a	1.11	1.20	1.09	1.00	0.80	0.83	0.77	0.72	0.43	0.67
4-Br	b	1.05	1.14	1.22	1.00	0.89	0.82	0.69	0.62	0.54	0.50
	a	1.15	1.08	1.21	1.00	0.87	0.88	0.74	0.70	0.49	0.45
3-F	b	1.20	1.24	1.03	1.00	0.96	0.86	0.80	0.70	0.58	0.70
3-Cl	b		1.13	1.03	1.00	0.91	0.97	0.82	0.86	0.58	0.64
4-NO_2	b	1.43	1.15	1.06	1.00	0.95	0.94	0.86	0.75	0.65	0.49
2-Me	b		1.14		1.00	1.17	1.08	1.21	1.15	1.32	1.42
2-F	b	1.28	1.02	0.94	1.00	0.94	0.90	0.80	0.76	0.78	0.75
	a	1.37	1.21	0.97	1.00	0.93	0.91	0.89	0.94	0.81	0.83

[a] Reaction in C_6H_6. [b] Reaction in CCl_4.

Table 2. Reaction constants (ρ) and correlation coefficients of the Hammett plots of the reaction rates in Table 1

Y	Solvent	ρ	*r*
4-Me	CCl_4	+0.386	0.922
	C_6H_6	+0.305	0.850
3-Me	CCl_4	+0.167	0.803
H	CCl_4	−0.167	0.751
	C_6H_6	−0.127	0.670
4-F	CCl_4	−0.241	0.854
	C_6H_6	−0.206	0.796
4-Cl	CCl_4	−0.251	0.909
	C_6H_6	−0.337	0.896
4-Br	CCl_4	−0.371	0.948
	C_6H_6	−0.413	0.976
3-F	CCl_4	−0.285	0.933
3-Cl	CCl_4	−0.278	0.966
4-NO_2	CCl_4	−0.404	0.991
2-Me	CCl_4	+0.117	0.828
2-F	CCl_4	−0.179	0.870
	C_6H_6	−0.167	0.870

calculations were carried out both on the free radicals and spin traps. From the calculations, it is revealed that both the HOMO and LUMO of the spin trap are π-orbitals delocalized mainly on the nitrone group and their LCAO coefficients on the benzylidene carbon atom are similar (Figure 2). In contrast, SOMOs of the aryl free radicals are σ-type orbitals and are localized on the free radical centre.[1,*] (The spin populations on the free radical's centre of occupied and unoccupied SOMOs are 0.54 and 0.71, respectively.) Therefore, the extent of overlap interaction and steric factors are expected to be nearly equal with the electron-transfer interactions both from the SOMO of free radical to the LUMO of the spin trap and from the HOMO of the spin trap to the SOMO of free radical. In general, the electron transfer is favourable when the energy difference between the interacting orbitals is small. Thus, the HOMO–LUMO pair† of the smaller energy differences should control the reactivity. The transition state is thus stabilized and the spin-trapping reaction is expected to be fast when the energy difference between the interacting HOMO and LUMO is small.[23,24]

The HOMO–LUMO energy difference is dependent on the substituent (Figure 3). In the reactions of the *p*-nitrophenyl free radical [Figure 3(a), in which $E_{lu}(R) - E_{ho}(T)$ is smaller than $E_{lu}(T) - E_{ho}(R)$], the rates are determined by $E_{lu}(R) - E_{ho}(T)$ and are expected to be favourable when the substituent (X) on PBN is electron-donating. In contrast, reactions of the *p*-tolyl free radical [Figure 3(d)] are controlled by $E_{lu}(T) - E_{ho}(R)$, and a positive ρ-value of the Hammett plot is predicted. Theoretical results are in accord with the observed kinetic substituent effect as shown in Figure 1. As expected from Figure 3(c), the reaction of unsubstituted phenyl free radicals towards X–PBNs are an intermediate example and the rather irregular plot in Figure 1 might be rationalized, though the plot appears rather convex in contrast to the prediction from MO calculations that it should be concave. The observed substituent effect is thus interpreted using the concept of HOMO–LUMO interaction and suggests the intermediary formation of a charge-transfer complex in the rate-determining stage of the reaction mechanism.

The substituent effect of the reaction of X–PBN with the *ortho*-substituted phenyl free radical is very similar to the same reaction with the *para*-substituted phenyl free radical. The SOMO energies of *ortho*-substituted phenyl free radicals are comparable to those of the corresponding MOs of the *para*-substituted phenyl free radical carrying the same substituent.‡

---

* Since the UHF calculation gives spin orbitals, the energy of the occupied spin orbitals of the SOMO is calculated to be considerably lower than the energy of the unoccupied spin orbital of the same MO. The former was taken as the SOMO energy when the electron-donating interaction with the LUMO of the spin trap was evaluated and, alternatively, the latter was taken as the SOMO energy when the electron-accepting interaction with the HOMO of the spin trap was evaluated.

† In the unified discussions of the HOMO–LUMO interaction, the occupied and the unoccupied spin orbitals were noted as the 'HOMO' and 'LUMO' of the free radical, respectively.

‡ For example, SOMO energies of 2- and 4-tolyl free radicals are −0.4003 and −0.3998 a.u., respectively, for occupied spin orbitals and are 0.0897 and 0.0899, respectively for unoccupied spin orbitals.

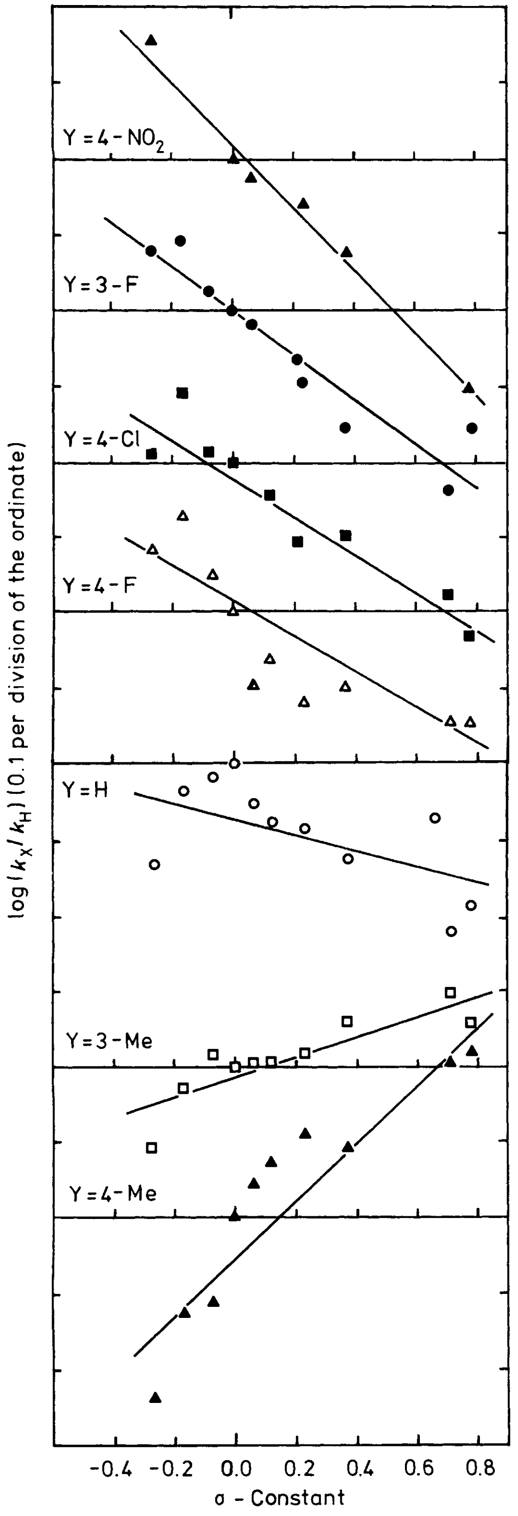

Figure 1. Plots of logarithms of the relative rates (k_X/k_H) *vs.* σ-constants of the substituents (X) on X–PBNs for a series of spin-trapping reactions

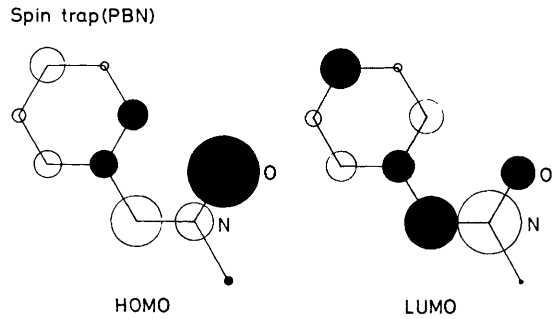

Figure 2. HOMO And LUMO of PBN

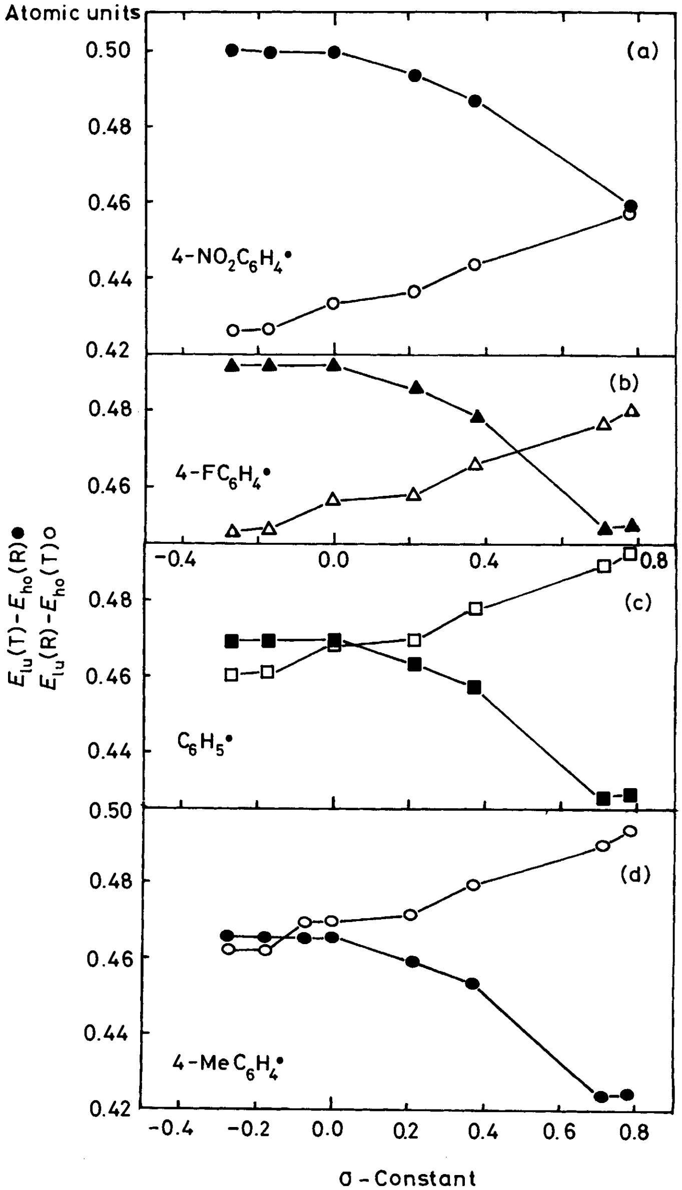

Figure 3. Substituent effect on the energy difference between LUMO and HOMO of the interacting spin trap (T) and free radical (R)*

* See footnote † on previous page.

Furthermore, the steric effect is eliminated throughout the series of reactions. Thus, the *ortho*-substituent effect is explained.

Open-shell INDO calculations on the model Me•–PBN system were carried out at various interatomic distances in an attempt to understand the reaction mechanism. For simplification, C-1(α)–N–C(Me_3) was fixed on the *xy* plane and C-2 (*i.e.* Me) of the attacking methyl free radical was assumed to lie on the *yz* plane. The interatomic distance (*d*) between C-1(α) and C-2 shortens as the reaction proceeds and can be used as a

Table 3. Optimized geometry and energy of the PBN–Me$^{\bullet}$ system as a function of the C-1 (PBN)–C-2(Me$^{\bullet}$) distance

d/nm	θ_1/deg	θ_2/deg	r_1/nm	r_2/nm	ΔE/kJ mol^{-1}
			0.132	0.125	0
0.40	97	107	0.132	0.126	13.2
0.35	98	108	0.134	0.126	−5.0
0.32	99	110	0.135	0.126	−17.7
0.28	100	108	0.136	0.126	−74.0
0.24	103	108	0.138	0.127	−177
0.22	105	106	0.139	0.126	−264
0.19	109	109	0.144	0.125	−441
0.151	114	112	0.148	0.124	−714

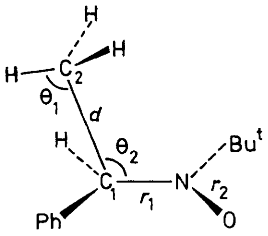

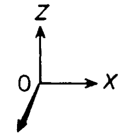

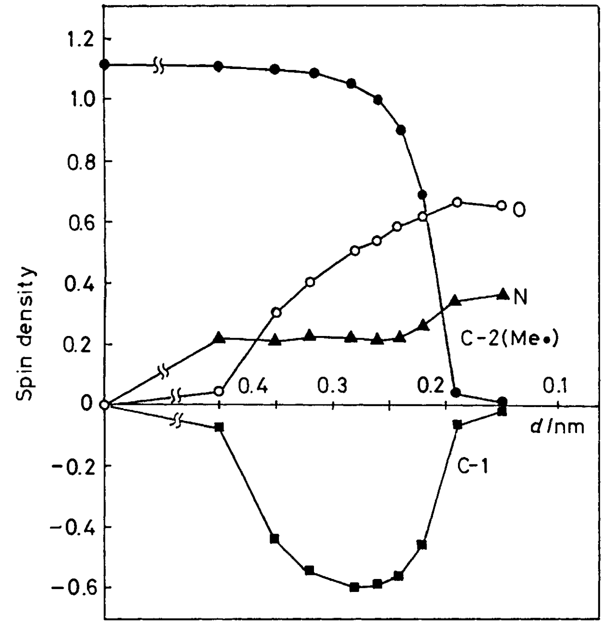

Figure 4. Spin migration during the process of the spin-trapping reaction

parameter to measure the progress along the reaction coordinate. Thus, the INDO–UHF calculations with optimization of geometry were carried out as a function of C-1–C-2 distance. The energy change (ΔE) of the system in reference to the isolated reactants (PBN and methyl free radical at $d = \infty$), and some of its geometrical parameters are given in Table 3.

A low energy barrier is predicted to exist when the methyl free radical is *ca.* 0.4 nm from the nitrone carbon atom (C-1). This implies that a low transition state forms at an early stage in the reaction mechanism. This hypothesis is reasonable when it is considered that the reaction involves a reactive free radical. Even when the methyl free radical is located less than 0.4 nm from the nitrone carbon atom, θ_1 is not 90° and the methyl group adopts a *ca.* pyramidal geometry. At this stage of the reaction, the unpaired electron orbital on the methyl carbon tends to mix with the LUMO of PBN (Figure 4). This again suggests the participation of an electron-transfer interaction between the 'HOMO' of the methyl group and the LUMO of PBN in the transition state. Since the methyl free radical is more electron-donating than aryl free radicals, this conclusion is reasonable and also in line with the LUMO energies of X–PBNs *vs.* their reactivities towards hex-5-enyl free radicals[10] (Figure 5).

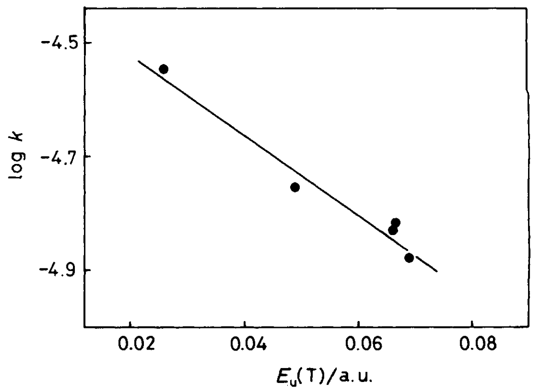

Figure 5. Plot of the logarithms of the rate constants of the reactions between hex-5-enyl and X–PBNs[19] *vs.* the LUMO energies of X–PBNs

However, the overlap population between C-1 and C-2 is rather small. Spin density on the methyl carbon atom does not decrease to a measurable extent until the C-1–C(2) distance (d) becomes less than 0.26 nm (Figure 4). Therefore, the spin density on the carbon, nitrogen, and oxygen atoms should be induced mainly by a through-space interaction. Rather abrupt changes in the C–N bond length and some bond angles occur when the C-1–C-2 distances becomes less than 0.24 nm. Formation of the σ-bond between C-1 and C-2 might proceed at this point in the reaction.

In summary, both the very low energy of activation[25] and the participation of electron-transfer stabilization in the transition state are reproduced by the MO calculations. Furthermore, the probable reaction path has been visualized.

Experimental

Preparation of Materials.—Substituted *N*-benzylidene-t-butylamine *N*-oxides were prepared from the corresponding substituted benzaldehydes following procedures utilized for the unsubstituted compound.[26,27] The intermediate *N*-benzylidene-t-butylamines, 3-aryl-2-t-butyloxaziranes, and the products were identified by their m.p.s, n.m.r., and mass spectra (Table 1). *N*-Benzylidene[$^2H_5$]aniline *N*-oxide was prepared from [$^2H_6$]benzene *via* *N*-[$^2H_5$]phenylhydroxylamine. Arylazotriphenylmethanes[28] were used as the source of aryl free radicals. The azo-compounds were synthesized by treating triphenylmethyl chloride with the corresponding arylhydrazine and by subsequent oxidation of the products by hydrogen peroxide. The products were characterized by routine spectroscopic measurement.

Reactions.—Aryl free radicals were generated by the thermal decomposition of the corresponding phenylazotriphenylmethanes. An excess (*ca.* 5 × 10^{-2} mol, each) of substituted *N*-benzylidene-t-butylamine *N*-oxide (X–PBN) and *N*-benzylidene[$^2H_5$]aniline *N*-oxide was added to a benzene or carbon tetrachloride solution of substituted phenylazotriphenylmethane (5.0 × 10^{-3} mol). In order to eliminate oxygen from the solution dry nitrogen was bubbled through for several min, and the solution was heated to 80 °C for 4 min. The spin-trapping reactions were terminated by this procedure. The coexisting

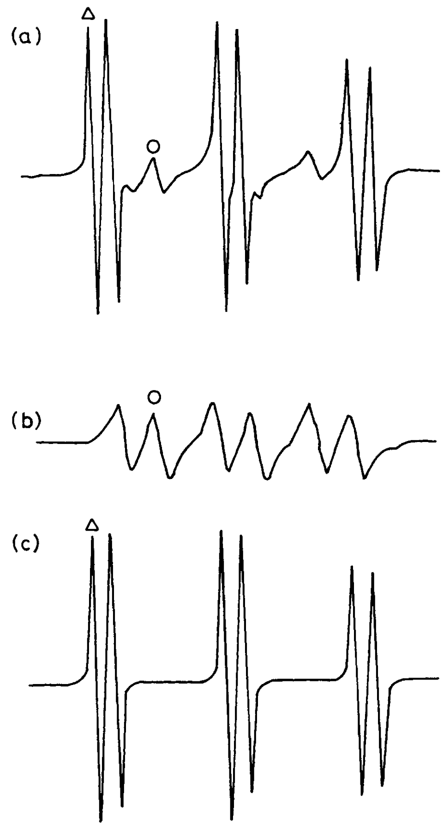

Figure 6. E.s.r. spectra of (a) the products of the competitive reaction, (b) the phenyl adduct of [$^2H_5$]DPN (a_N = 10.9, *G*, a_H = 3.5 *G*), and (c) the phenyl adduct of PBN (a_N = 15.0 *G*, a_H = 2.4 *G*)

triphenylmethyl free radical was scavenged by passing gaseous oxygen through the solution.

Measurement of E.S.R. Spectra.—E.s.r. spectra were measured on a JEOL JES-ME-3X spectrometer. The product from the spin-trapping reaction was placed in a capillary tube (φ 1.5 mm × 15 cm, manufactured by Clay Adams and Co.), which was then inserted into an e.s.r. sample tube. The *g*-values and hyperfine splitting constants were obtained with reference to the Mn^{2+} lines. Concentrations of the free radicals were also determined by use of a calibration line preliminarily drawn with stable 4-hydroxy-2,2,6,6-tetramethylpiperidine-*N*-oxyl free radical solution in reference to 1M aqueous $MnCl_2$ solution.

Determination of Relative Rates by E.S.R. Spectroscopy.—In order to determine the relative rate constant k_1/k_2 [in equation (3)], the e.s.r. spectrum of the reaction mixture was measured after scavenging the triphenylmethyl free radical. Spectral lines of DPN and PBN adducts overlap each other considerably [see Figure 6(a)]. However, the line at the lowest frequency (marked by the triangle) of the PBN adduct does not overlap with any line of the [$^2H_5$]DPN adduct [Figure 6(b)]. Thus its intensity was compared with that of the second lowest line (marked by the circle) of the [$^2H_5$]DPN adduct which is also separated from the lines of PBN adduct [Figure 6(c)]. The concentrations of the spin adducts were assumed to be proportional to the intensity measured as the peak-to-trough separation of the spectral line. The absolute intensity of each line had been determined preliminarily by using the calibration lines.

A series of four runs carried out by using unsubstituted PAT and PBN gave k_1/k_2 4.34 ± 0.08, which lead to the standard deviation of *ca.* 2%. All k_1/k_2 ratios were determined similarly by averaging the data collected from three to five runs. Thus the error for k_X/k_H values should be *ca.* 4%.

Molecular Orbital Calculations.—CNDO/2 And INDO molecular orbital calculations were carried out by use of TLIBY Y4CBO4N library programme of the Computer Centre of the University of Tokyo. The computer programme is a slightly modified version of that originally developed by Pople and co-workers.[29,30]

Acknowledgements

We thank Professor Tokuko Watanabe and Professor Jiro Higuchi (Yokohama National University) for their valuable advice and the latter for his kind permission to use a JEOL JES-ME-3X ESR spectrometer. INDO MO Calculations were carried out by HITAC M-200H computers of the Institute for Molecular Science and, in part, of the University of Tokyo to which the authors are grateful. This research was supported by a Grant-in-Aid for Scientific Research from the Ministry of Education, Science and Culture of Japan.

References

1 W. A. Waters, 'Chemistry of Free Radicals,' Oxford University Press, London, 1946.
2 C. Walling, 'Free Radicals in Solution,' John Wiley and Sons, New York, 1957.
3 E. G. Janzen and B. J. Blackburn, *J. Am. Chem. Soc.*, 1968, **90**, 5909.
4 E. G. Janzen and B. J. Blackburn, *J. Am. Chem. Soc.*, 1969, **91**, 4481.
5 E. P. Sargent and E. M. Gardy, *Can. J. Chem.*, 1976, **54**, 275.
6 G. R. Buttner, L. W. Oberley, and S. W. H. C. Leuthauser, *Photochem. Photobiol.*, 1978, **28**, 693.
7 T. Kunitake and S. Murakami, *J. Polym. Sci., Polym. Chem. Ed.*, 1974, **12**, 67.
8 E. G. Janzen, *Acc. Chem. Res.*, 1971, **4**, 31.
9 C. Lagercrantz, *J. Phys. Chem.*, 1971, **75**, 3466.
10 P. Schmid and K. U. Ingold, *J. Am. Chem. Soc.*, 1978, **100**, 2493.
11 R. W. Henderson and R. D. Ward, Jr., *J. Am. Chem. Soc.*, 1974, **96**, 7556.
12 W. A. Pryor and W. H. Davis, Jr., *J. Am. Chem. Soc.*, 1974, **96**, 7557.
13 R. W. Henderson, *J. Am. Chem. Soc.*, 1975, **97**, 213.
14 A. A. Zavitsas and G. M. Hanna, *J. Org. Chem.*, 1975, **40**, 3782.
15 A. A. Zavitsas and J. A. Pinto, *J. Am. Chem. Soc.*, 1972, **94**, 7390.
16 M. Kamimori, H. Sakuragi, T. Suehiro, K. Tokumaru, and M. Yoshida, *Bull. Chem. Soc. Jpn.*, 1977, **50**, 1195.
17 M. Kamimori, H. Sakuragi, K. Sawatari, T. Suehiro, K. Tokumaru, and M. Yoshida, *Bull. Chem. Soc. Jpn.*, 1979, **52**, 2339.
18 P. I. Abell, *Trans. Faraday Soc.*, 1964, **60**, 2214.
19 C. L. Greenstock and R. H. Wiebe, *Can. J. Chem.*, 1982, **60**, 1560.
20 L. P. Hammett, *J. Am. Chem. Soc.*, 1937, **59**, 96.
21 D. H. McDaniel and H. C. Brown, *J. Org. Chem.*, 1958, **23**, 420.
22 M. M. Martin and G. J. Gleicher, *J. Am. Chem. Soc.*, 1964, **86**, 233 and 242.
23 G. Klopman and R. F. Hudson, *Tetrahedron Lett.*, 1967, 1103; *Theor. Chim. Acta*, 1967, **8**, 165.
24 G. Klopman, *J. Am. Chem. Soc.*, 1968, **90**, 233.
25 T. Suehiro and M. Ishida, *Bull. Chem. Soc. Jpn.*, 1971, **44**, 1692.
26 B. L. Emling, *J. Org. Chem.*, 1959, **24**, 657.
27 W. D. Emmons, *J. Am. Chem. Soc.*, 1957, **79**, 5739.
28 S. Solomon, C. H. Wang, and S. G. Cohen, *J. Am. Chem. Soc.*, 1957, **79**, 4104.
29 J. A. Pople, D. L. Beveridge, and P. A. Dobosh, *J. Chem. Phys.*, 1967, **47**, 2062.
30 J. A. Pople and G. A. Segal, *J. Chem. Phys.*, 1966, **44**, 3289.

Received 13*th November* 1986; *Paper* 6/2182